Stray Light and Atmospheric Adjacency Effects for Large-FOV, Ocean Viewing Space Sensors

Kendall L. Carder

University of South Florida, 140 7th Avenue S, St. Petersburg, Florida 33701

kcarder@marine.usf.edu

Monte Carlo Simulations

Hole in the Cloud

1. The hole in the clouds is a 3-D problem requiring Monte Carlo simulation of the atmospheric adjacency. It demostrates how clouds affect downwelling irradiance at the sea surface. (FIG 1) All calculations use Elterman's (1968) atmosphere with water Fresnel reflectance and about a 2% diffuse reflectance

2. $E_{sky\_d}(550)/F_0(550)$ for sky hole (radius) in clouds with 40° solar zenith angle as observer moves away from hole center. (FIG 2)

NOTE that $E_{sky\_d}(550)/F_0(550)=0.28$ for a "no-cloud" scenario and 0.33 near the hole center. The clouds can increase downwelling irradiance from the sky by 18% even when they are 5 km away. Similiar 3-D problems must be dealt with in evaluating adjacency effects in upwelling radiance.

Dark target /Bright Surround

1. The dark target/bright surround is similar to a lake of 5 km radius surrounded by a region bright reflectivity (50%).

NOTE: The dark target calculation in Fig. 2 shows that proximity to land does not effect $E_{sky\_d}(550)$. The 2-D dark target problem is much simpler than the cloud problem.

To evaluate stray light problems on satellite sensors, dark targets like lakes or ocean areas surrounded by bright land or shoal regions are much easier to correct for atmospheric adjacency effects than are holes in clouds. (See Reinersman et al., 1995)

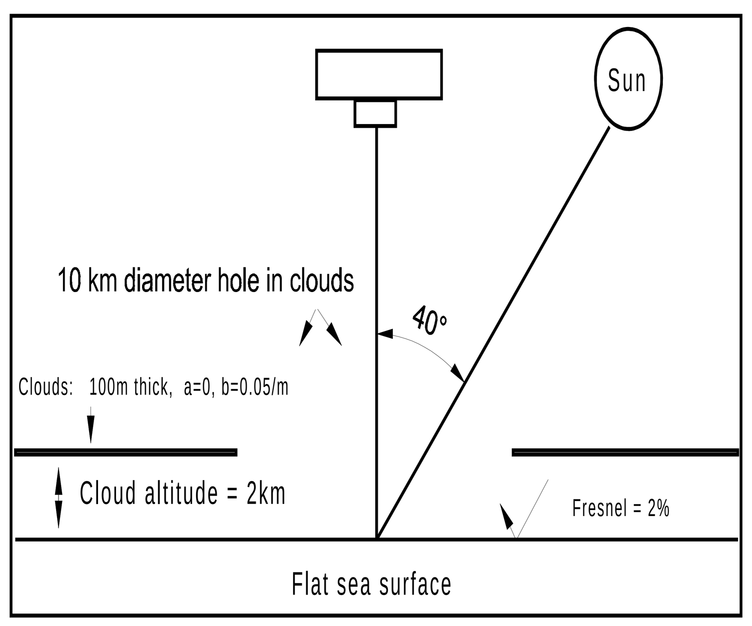

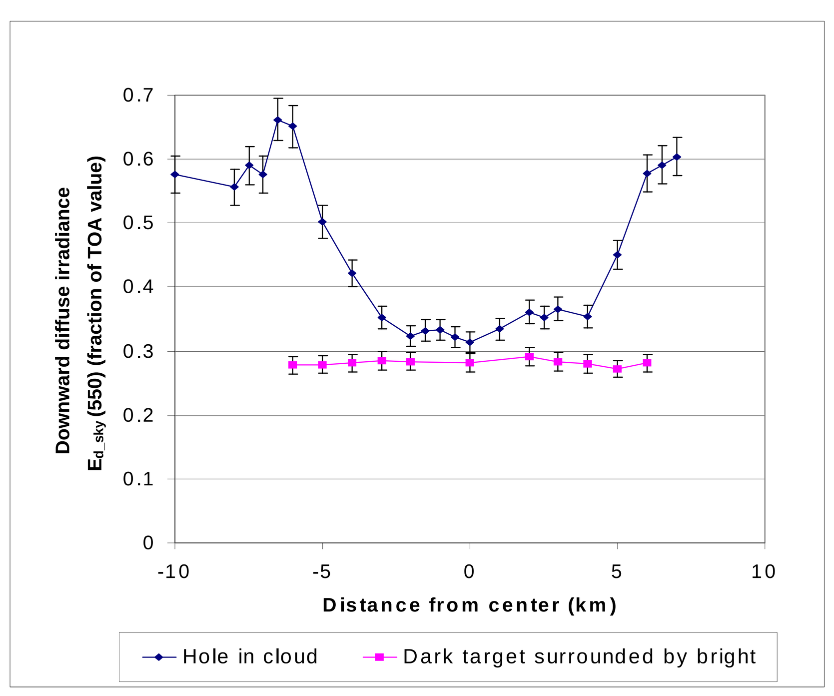

Dark Target Surrounded by Brighter Reflectance Tongue of the Ocean TOTO

1. Shallow banks still present a uniformly dark target in the infrared, so atmospheric correction is not compromised for SeaWiFS.

2. Relatively high contrast is observered at blue-green wavelengths where shallow, bright carbonate banks are adjacent to deep, clear water that are horizontally uniform at 510nm & 550 nm. FIGURE 3 & 4.

3. Reinersman et al. (1995) showed that atmospheric adjacency effects of land on the adjacent water views were only significant within about 1 to 2 km of land in the infrared. Rayleigh-contributed adjacency effects will be greater at 510 and 550nm, so more is expected at TOTO.

4. AVIRIS imagery and Monte Carlo simulations to evaluate TOTO adjacency effects as in Reinersman et al. (1995). Significant residuals in SeaWiFS will be considered to be stray light.

Methods for correcting adjacency and stray light effects will be explored.

Figure 3. SeaWiFS False color over south Florida and the Bahamas

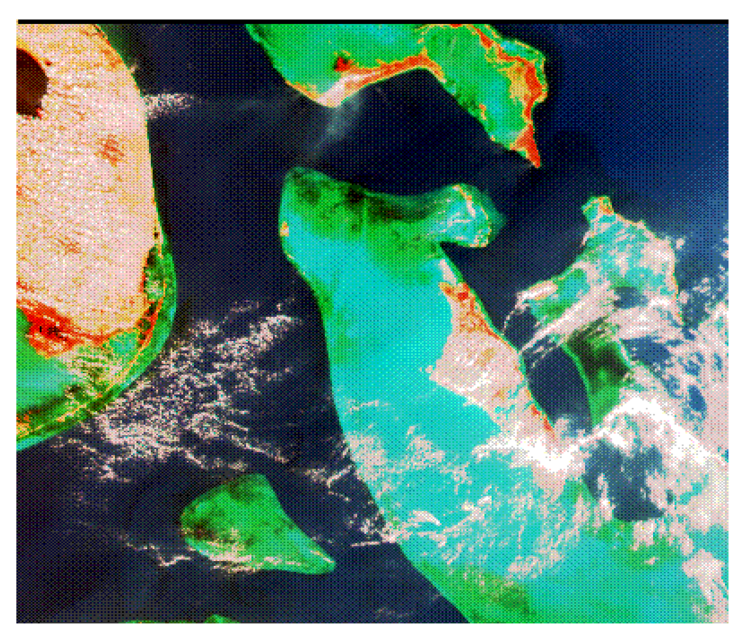

Northwest Passage of the Tongue of the Ocean, Bahamas

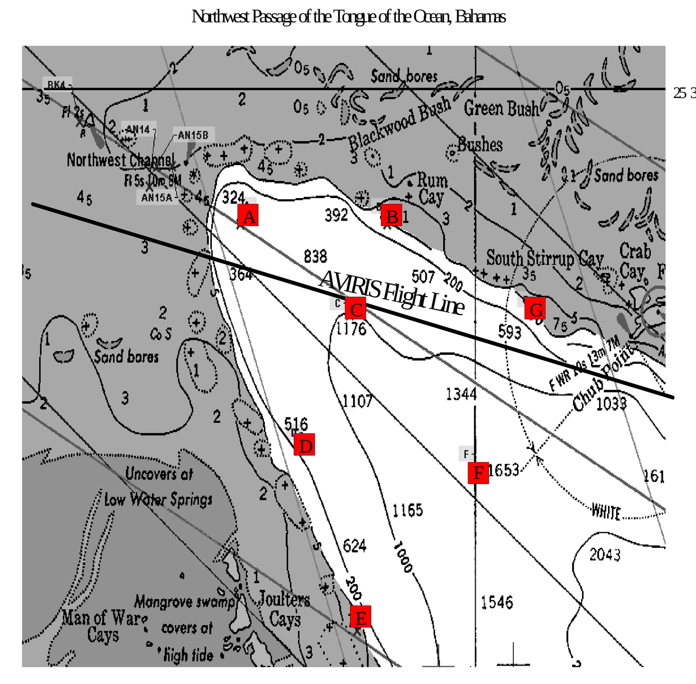

Figure 5. Rrs(555) for TOTO. Pixels are about 1 km apart. Red Crosses are field values at sites A, C, F. Stars are from SeaWiFS.

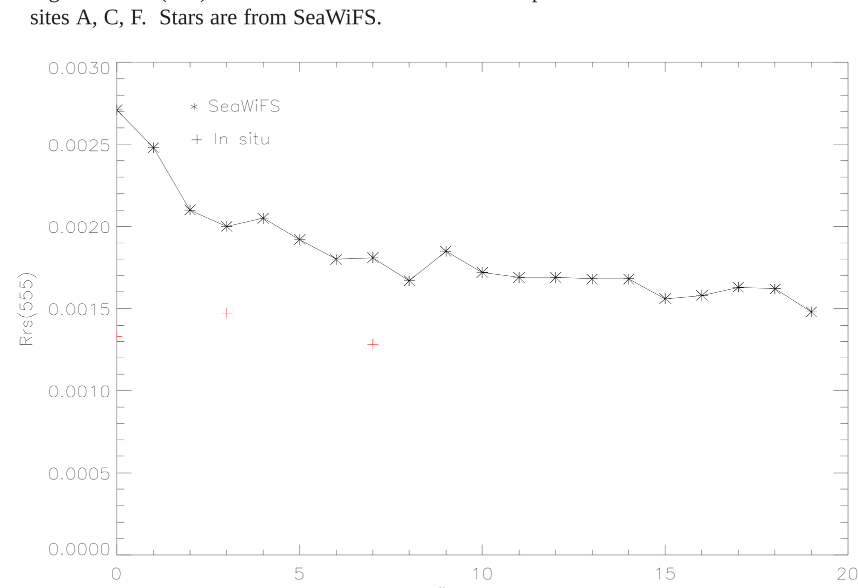

Applications

To reach the point where we believed that SeaWiFS would provide year-to-year consistency in data quality, we performed an evaluation of SeaWiFS calibration and algorithm performance.

1. SeaWiFS performance in the Sargasso using bands 6&8 for atmospheric correction (Hu et al. 1999). (FIGURE 6.) Note that Lw(555) field is now much closer to 0.28 mW/cm2/um/ster.

1. Performance in the turbid coastal zone has been enhanced using the aerosol type from adjacent, non-turbid waters. Note the significant increase in non-negative pixels and reduction in chl-a value for turbid waters. (Hu et al. 1999) FIGURE 7.

2. SeaWiFS performance in TOTO and Florida shelf water using the Carder et al. (1999) chl-a and CDOM algorithms were checked. Chl-a retrieved using the SEADAS and Carder algorithms were within 5% for Case 1 waters but for CDOM-rich waters Carder results were within 25% of measured data while SEADAS were high by as a factor of four (included in Carder 1998 SIMBIOS final report). FIGURE 8a&b

Evaluation of SeaWiFS sensitivity to stray light at visible wavelengths
Ship, SeaWiFS, and AVIRIS data were collected during April-May in the Northwest Passage of the Tongue of the Ocean, Bahamas. FIGURE 5. where SeaWiFS Rrs(555) values progressively increased over deep water with proximity to the head of the Passage. FIGURE 4. Rrs(555) values in the open waters 20 km from the Passage were close to the Gordon and Clark (1981) clear water values of 0.0015 (nLw(550)≈0.28 mw/cm2/um/ster);

Figure 6.

Atmospheric correction of SeaWiFS imagery: assessment of alternative bands
Chuanmin Hu, Kendall L. Carder, Frank E. Muller-Karger
submitted to *Appl. Opt.* July 1999

Over uniform oligotrophic waters such as the Sargasso Sea, Band 6 performs better than Band 7 in terms of retrieving homogeneous nLw_555 and chlorophyll-*a* concentration, especially when perturbation exists in the total signal, possibly caused by high-altitude aerosols or thin cirrus clouds (e.g., the vicinity of the rectangular box). The cloud-detection algorithm in the default NASA algorithms (SeaDAS) doesn't detect thin cirrus. Digitization-caused errors are also reduced by using Band 6 in the atmospheric correction. A sample comparison for the SeaWiFS scene over the Sargasso Sea on April 4, 1998 is shown here. For this location nLw_555 should be constant and ~0.27 $mW \cdot cm^{-2} \cdot \mu m^{-1} \cdot sr^{-1}$. Top: default nLw_555 (using Bands 7 and 8 in the atmospheric correction); Bottom: nLw_555 by using Bands 6 and 8 in the atmospheric correction. Note that values larger than 0.5 are clouds, and values between 0.35 and 0.5 are likely thin cirrus or cloud-adjacency effects, which are markedly reduced in the bottom figure vs. the top figure.

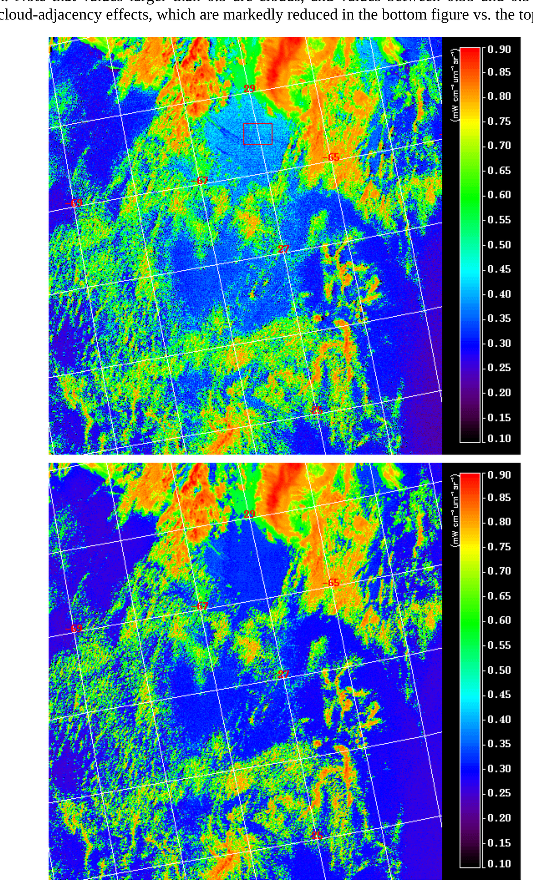

Figure 7.

Atmospheric correction of SeaWiFS imagery over turbid coastal waters: a practical method
Chuanmin Hu, Kendall L. Carder, and Frank Muller-Karger
submitted to *Remote Sensing of Environ.* June 1999

The method applies "borrowed" aerosol type over coastal waters based on "nearest neighbor". A sample correction result for the SeaWiFS scene over the Northeast Gulf of Mexico on April 10, 1998 is shown here. Top: default chlorophyll-*a* concentration; Bottom: chlorophyll-*a* concentration after the coastal correction. Note that chlorophyll-*a* concentration decreases in the coastal area, and areas with the atmospheric-correction failure mask are often successfully recovered.

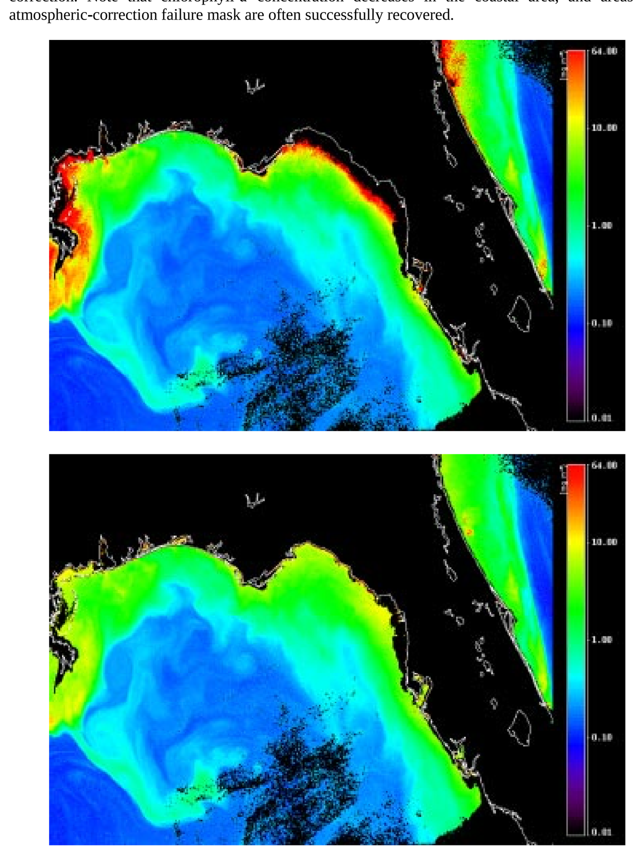

Figure 8a. ag(400) April 3, 1998

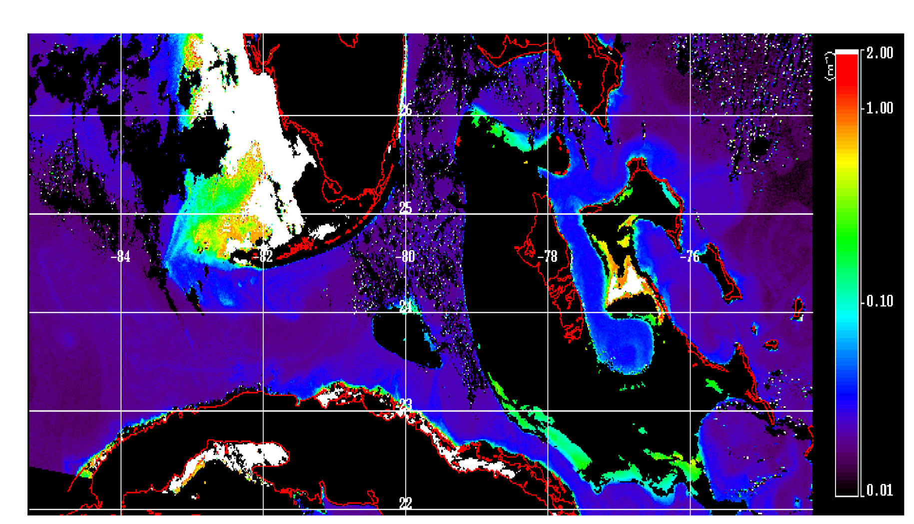

Figure 8b. ag(400) April 14, 1999

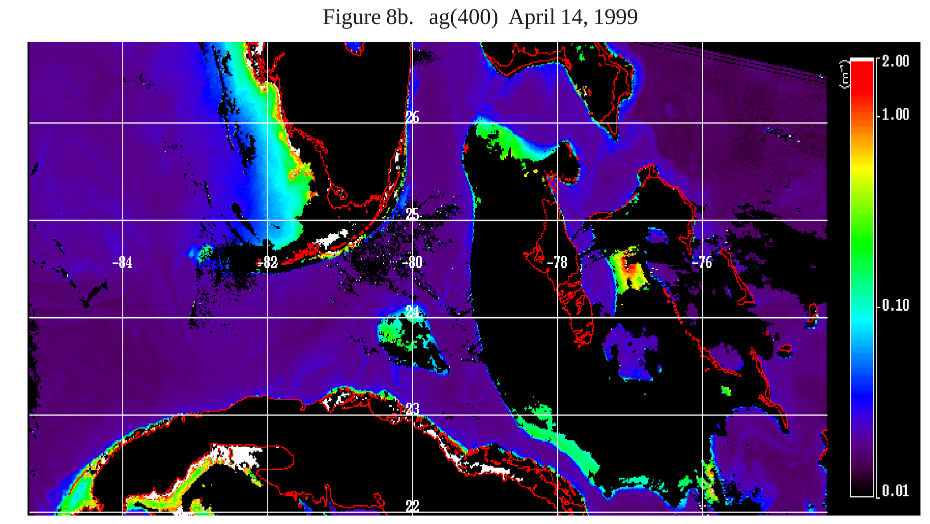

Figure 9.

AVIRIS quicklook images at 500nm

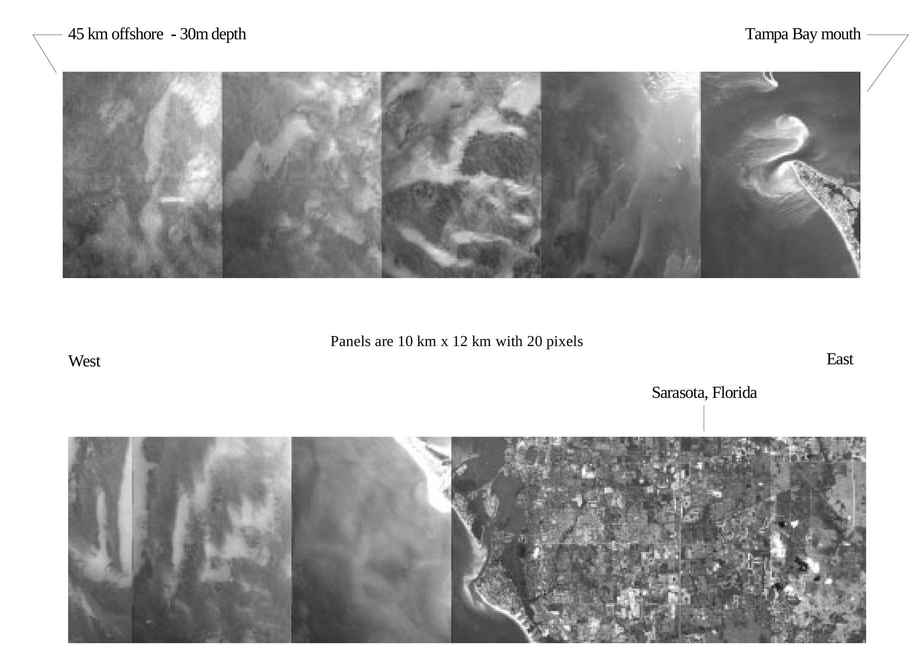

Publications

Bissett, W.P., J.J. Walsh, D.A. Dieterle, K.L. Carder. 1999. Carbon cycling in the upper waters of the Sargasso Sea: I. Numerical simulation of differential carbon and nitrogen fluxes, Deep Sea Res. (46)2: 205-269.

Bissett, W.P., K.L Carder, J.J. Walsh, D.A. Dieterle. 1999. Carbon cycling in the upper waters of the Sargasso Sea: II. Numerical simulation of apparent and inherent optical properties, Deep Sea Res. (46)2: 271-317.

Carder, K.L., F.R. Chen, Z.P. Lee, S.K. Hawes, D. Kamykowski. 1999. Semianalytic Moderate Resolution Imaging Spectrometer algorithms for chlorophyll a and absorption with bio-optical domains based on nitrate-depletion temperatures. Journal of Geophys. Res. 104(C3): 5403-5421.

D'Sa, E.D., J.B. Zaitzeff, and R.G. Steward, (submitted). Monitoring water quality in Florida Bay with remotely sensed salinity and in situ bio-optical observation. International Jour. of Remote Sensing.

D'Sa, E.D., R.G. Steward, A. Vodacek, N.V. Blough, D. Phinney. 1999. Determining optical absorption of colored dissolved organic matter in seawater with a liquid capillary waveguide. Limnol. Oceanogr. 44(4): 1142-1148.

D'Sa, E.J., J.B. Zaitzeff, and R.G. Steward. (in press) Remote salinity and ocean color monitoring: Aspects and performance in a coastal environment. In International Conference on Satellite, Oceanography, and Society. Ed. D. A. Halpern.

Hu, C., K.L. Carder, and F. Muller-Karger. Atmospheric correction of SeaWiFS imagery over turbid coastal waters: a practical method, submitted to Remote Sensing of Environ. June 1999

Hu, C., K.L. Carder, and F. Muller-Karger. Atmospheric correction of SeaWiFS imagery: assessment of alternative bands, submitted to Appl. Opt. July 1999

Lee, Z.P., K.L. Carder, C.D. Mobley, R.G. Steward, and J.S. Patch. 1999. Hyperspectral remote sensing for shallow waters. 2. Deriving bottom depths and water properties by optimization. Applied Optics 38(18): 3831-3843.

Reinersman, P.R. and K.L. Carder. 1995. Monte Carlo simulation of the atmospheric point spread function with an application to correction for the adjacency effect. Appl. Opt. 34:4453-4471.

Reinersman, P.R., K.L. Carder, and F.R. Chen. 1998. Satellite sensor calibration verification with the cloud shadow method. Appl. Opt. 37:5541-5549.

Zaitzeff, J.B., E.J. D'Sa, C.S. Yentsch, J.L. Miller, R.G. Steward, R. Ives. (in press) Rapid remote assessments of salinity contrasts in Florida Bay and bio-optical variability. In Linkages Between Ecosystems in the South Florida Hydroscape: The River of Grass Continues. (Eds) J.W. Porter and K.G. Porter.

Other References

Gordon, H.R. and D.K. Clark. 1981. Clear water radiances for atmospheric correction of coastal zone color imagery. Appl. Opt. 20: 4175-4180.